A Comparative Study of Digital Filtering Techniques in Ultrasound and Carotid Bifurcation Atherosclerosis

Adriana MILĂȘAN, Cristian MOLDER, and Silviu DUMITRESCU

***Abstract*—The current paper presents a method for speckle cancellation in digital images obtained in ultrasound and carotid bifurcation atherosclerosis. Filtering techniques are usually used for noise reduction and contrast enhancement in digital images. Due to interferences and other phenomena in the acquisition chain, ultrasound images usually have perturbations and artifacts. Speckle is often considered a powerful source of noise in the ultrasound imagery and it must be filtered without affecting the rest of the most important features in the image. Linear, nonlinear, diffusion and wavelet filters are applied on various ultrasound images of carotid bifurcation. In order to evaluate the quality difference between original and anti-speckle filtered images, a comparative study of results is presented at the end.**

***Index Terms*—Ultrasound, carotid bifurcation, speckle, filtering.**

I. Introduction

Enhancement algorithms are used to noise reduction in digital images and for contrast enhancement of regions of interest. In images with rather close aspects of normal and abnormal tissues, a positive interpretation can sometimes be a difficult task due to higher relative noise levels. In most situations, this step allows the enhancement of the image quality and eases diagnosis. Enhancement techniques are usually used to provide a much clearer image to the human observer. At the same time, they can be viewed as a preprocessing step in an automatic analysis processing chain.

If incorrectly used, the enhancement techniques can increase the noise level while enhancing the image contrast, can remove small details and contour clarity while canceling the noise, and can produce artifacts.

Ultrasound images generally have a lower signal-to-noise ratio mainly due to three sources. First, ultrasound scanners use short-time pulsed signals which is equivalent to a wide spectrum. Therefore, signals can be affected by multiple noise sources. Second, the coherent nature of signals generates speckle noise. Third, soundwaves are highly distorted when travelling through tissues. Therefore, ultrasound images can have various types of artifacts that can affect their quality. Speckle examples are shown in Figures 1 and 2 [1].

Figure 1 shows the presence of a phantom in a mammary tissue disposed in a water tank, while Figure 2 shows contrast phantoms in hypoechoic mass and a metallic pin within a water tank. The artifacts observed in these images distort shape and texture and hide details. Ultrasound artifacts can be classified in three classes: wave propagation artifacts, attenuation artifacts and sound speed artifacts.

Speckle appears when targets are scanned below pulse resolution and independent phase front waves are cumulating. This phenomenon can be geometrically described as a random displacement of component phasors [2], [3]. Scattering from targets within the resolution cell is influenced by constructive and disruptive interferences which lead to intensity fluctuations in the image, therefore degrading its quality.

Filtering Techniques Speckle artifacts in ultrasound imaging is sometimes called noise or tissue texture. Despite, the speckle is not a conventional noise, because the artifact template is identical for a series of images of a stationary object. Noise would have a random pattern, while the RF means value will cancel this noise. The speckle is present even if the mean of images is computed. Therefore, the speckle presence does not characterize a tissue feature but rather an ultrasound feature.

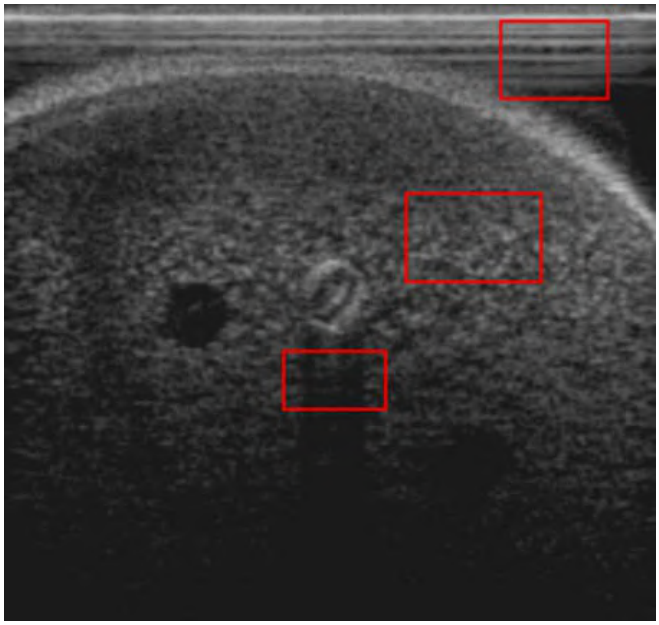

Figure 1. Phantom of a mammary ultrasound image with multiple artifacts. The enclosed regions show examples of artifacts. Top: reverberations. Middle: speckle. Bottom: shadowing

A. Milășan is with the Center of Excellence in Robotics and Autonomous Systems, Laboratory of Robotics, Military Technical Academy, 39-49 George Coşbuc Ave., Sector 5, 050141, Bucharest, Romania (e-mail: adriana.milasan@mta.ro).

C. Molder is with the Center of Excellence in Robotics and Autonomous Systems, Laboratory of Robotics, Military Technical Academy, 39-49 George Coşbuc Ave., Sector 5, 050141, Bucharest, Romania (e-mail: cristian.molder@mta.ro).

S. Dumitrescu is with the "Dr. Carol Davila" Central Military Emergency University Hospital, 134 Calea Plevnei Ave., Sector 1, 010825, Bucharest, Romania (e-mail: dr.silviu.dumitrescu@gmail.com).

Digital Object Identifier 10.32754/JMT.2018.1.01

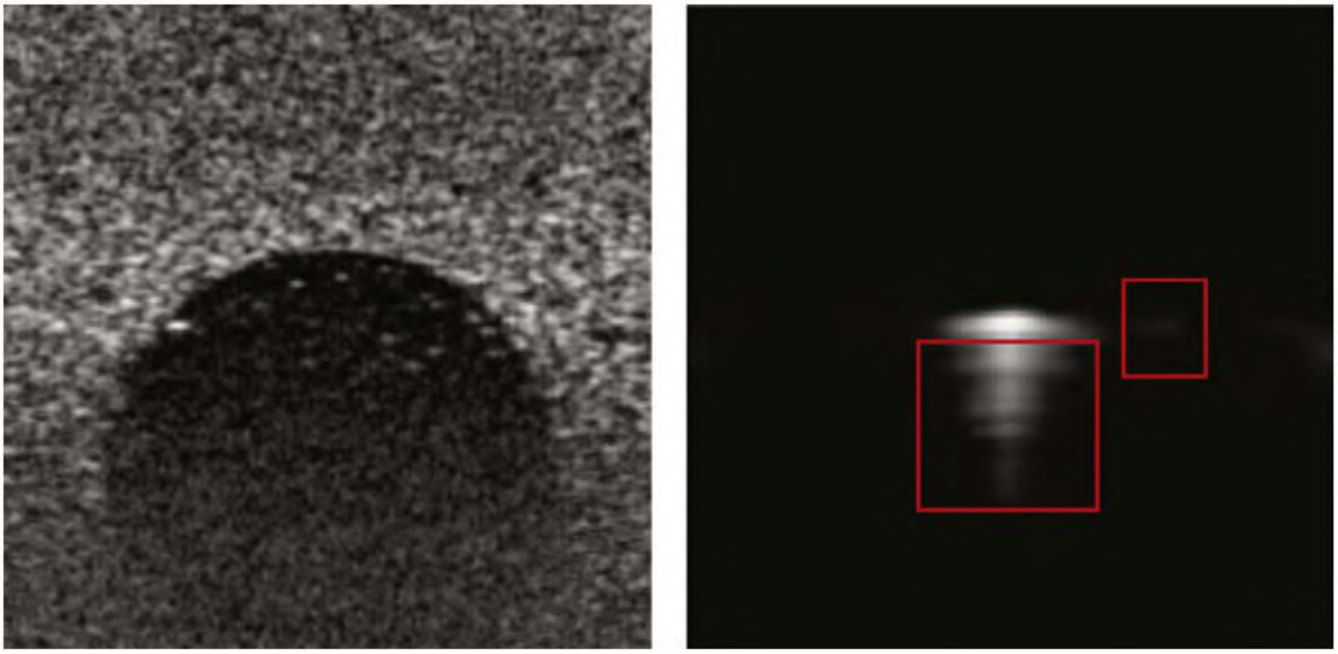

a) *b)*

Figure 2. a) Hypoechoic mass inside a contrast phantom, b) Metallic pin inside a water tank. The comet tail appears below and the side lobe on the right

II. FILTERING TECHNIQUES

Large scale use of ultrasound imagery equipment, including mobile and handheld ultrasound scanning devices, as well as computer aided systems, all require better image processing techniques in order to provide clear images to the medical experts. Therefore, the use of an efficient anti-speckle filtering is an important task. The speckle is not technically a true noise as its textural features can often provide useful data related to the analyzed image.

The speckle limits the efficient use of image processing and analysis (e.g. contour detection, segmentation) and 2D display or 3D volume rendering. Therefore, the speckle is often considered a powerful source of noise in the ultrasound imagery and it must be filtered without affecting the rest of the most important features in the image.

Table I presents the anti-speckle filtering techniques related to this study, classified into four categories: linear filtering (local statistics filters, homogeneous filters), non-linear filtering (median filters, linear scale filters, geometric filters, logarithmic filters, homomorphic filters), anisotropic diffusion filtering (anisotropic filters, reduced speckle anisotropic filters, non-linear coherent anisotropic filters), and wavelet filtering. Used techniques and author references are also described.

To obtain an efficient anti-speckle filter a speckle noise model is required. In the context of ultrasound images the speckle noise model can be approximated as a multiplicative noise. The demodulator output signal the imagery receiver can be defined as follows:

$$y_{i,j} = x_{i,j} n_{i,j} + a_{i,j} \quad (1)$$

where $y_{i,j}$ is the noised pixel at the center of the sliding window, $\log\left(y_{i,j}\right) = \log\left(x_{i,j}\right) + \log\left(n_{i,j}\right)$ is the noise free pixel, $n_{i,j}$ and $a_{i,j}$ are the multiplicative and additive noises, and i, j are spatial location indexes in the 2D real domain $i, j \in R^2$. Logarithmic compression is applied to the detected echo envelope to normalize display [4], [5]. It has been proven that logarithmic compression affects the speckle noise statistics such as the local mean becomes proportional to the local variance rather than the standard deviation [6]. The logarithmic compression affects the higher intensities of the probability density function more than in its lower intensities. Therefore, the speckle noise becomes close to a white Gaussian noise which is related to the uncompressed Rayleigh signal [5]. Considering that the additive noise effect is considerably lower than the effect of the multiplicative noise, (1) can be rewritten as follows:

$$y_{i,j} \approx x_{i,j} n_{i,j} \quad (2)$$

The logarithmic compression changes the model defined by (2) into a classic signal with additive noise:

$$log\left(y_{i,j}\right) = log\left(x_{i,j}\right) + log\left(n_{i,j}\right) \quad (3a)$$

$$g_{i.j} = f_{i.j} + nl_{i.j} \quad (3b)$$

The $log\left(y_{i,j}\right)$ term corresponding to the current observed pixel of the ultrasound image that is shown on display after the logarithmic compression further noted as $g_{i.j}$, while $log\left(x_{i,j}\right)$ and $log\left(n_{i,j}\right)$ terms corresponding to the noise free pixel and the logarithm noise component, are further noted as $f_{i.j}$ and $nl_{i.j}$, respectively (see (3b)).

A. Linear Filters

Most despeckle filtering techniques referred in the literature use local statistics. The algorithm can be described as a weighted mean that is using local statistics to estimate statistical measures on various pixel windows sizes, from 3×3 to 15×15 pixels. These techniques consider the speckle as multiplicative noise, such as presented in (1).

1) Linear despeckle filter

Filters using first order statistics such as mean and variance can be modeled using (1). Therefore, algorithms of this class can be traced back to the following equation:

TABLE I. GENERAL OVERVIEW OF SPECKLE NOISE CANCELLING FILTERS

Filter class	Algorithm	References
Linear filtering	Sliding window with local statistics:	
	(a) mean, variance	[8], [15]
	(b) homogeneous mask local filter	[8], [10], [19]
	(c) Wiener	[8], [14]
Non-linear filtering	Median filter	
	Filter based on the most homogeneous neighbor pixel	[8], [10], [15]
	Geometric filter	[8], [10], [11]
	Logarithm, FFT, noise cancelling, inverse FFT, exponential	[8], [15], [16]
Diffusion filtering	Nonlinear filtering for simultaneous contrast enhancement and noise reduction	[7], [8], [10], [12], [13]
	Diffusion with coherence enhancement	[8], [10]
Wavelet filtering	Use of most significant wavelet coefficients	[10], [14]

$$f_{i,j} = \overline{g} + k_{i,j}\left(g_{i,j} - \overline{g}\right), \tag{4}$$

where $f_{i,j}$ is an estimated value of a noise free pixel, $g_{i,j}$ is the noisy pixel from the sliding window, $\overline{g}$ is the local mean of the neighbor region $N_1 \times N_2$, including the pixel $g_{i,j}$, $k_{i,j}$ is a weighting coefficient, with $k \in [0...1]$, while i, j are the pixel coordinates. Weight $k_{i,j}$ is a function of local statistics inside a sliding window, that can be found under various expressions [9,10]:

$$k_{i,j} = \frac{1 - \overline{g}^2\sigma^2}{\sigma^2\left(1+\sigma_n^2\right)+\sigma^2} \tag{5}$$

$$k_{i,j} = \frac{\sigma^2}{\overline{g}^2\sigma_n^2 + \sigma^2} \tag{6}$$

$$k_{i,j} = \frac{\sigma^2 - \sigma_n^2}{\sigma^2} \tag{7}$$

Values of σ^2 and σ_n^2 are variances inside the sliding window and of the entire image, respectively. Noise variance is obtained from the logarithmic compressed image by computing the noise mean variance in windows considerably larger than the filtering window. If $k_{i,j}$ is 1 (contour regions), the pixel value remains unchanged, while a 0 (uniformity) replaces the current pixel with the local mean $\overline{g}$ in the region of interest (see (4)). The despeckle filter uses a 5×5 pixel sliding window size.

2) Homogeneous mask local filter

This is a 2D filter that is applied in a 5×5 pixels matrix searching for the most homogeneous region neighboring each pixel using a sliding sub-window of 3×3 pixels. The central pixel of the 5×5 pixels region is replaced by the mean gray level of the 3×3 pixels mask which has the lowest speckle index C, where C is considered for logarithmic compressed images:

$$C = \frac{\sigma_s^2}{\overline{g}_s} \tag{8}$$

where σ_s^2 and $\overline{g}_s$ are the variance and mean of the 3×3 window, respectively. The window with the lowest C is the most homogeneous sub-window which, most probably, does not contain any contour. The sliding window size for this filter is 5×5 pixels.

B. Nonlinear Filters

1) Median filter

The median filter is a simple nonlinear operator which replaces the central pixel in a window by the median value of its neighbors. The sliding window size is 7×7 pixels.

2) Filter based on the most homogeneous neighbor pixel

This type of 1D filter operates in a 5×5 pixels window and looks for the most homogeneous region in the neighborhood of each pixels of the image. The central pixel from the 1×5 vicinity is then replaced by the gray level intensity of the 1×5 pixels mask. The filter is iteratively applied to the image, the number of iterations being selected by the user. This filter does not require parameters or thresholds and is suitable for automatic processing.

3) Geometric filter

The geometric filtering is based on the fact that the speckle is present in images as rapid high and low intensity changes. The geometric filter - using iterations - attenuates the extreme intensities, keeping weak intensities unchanged. The filter used in the study uses a nonlinear noise canceling by comparing the central pixel value of a 3×3 window with its eight surrounding neighbors and, based on their intensities, rises or lowers the central pixel intensity.

4) Homomorphic filter

A homomorphic filter $H(\cdot)$ can be designed either by using a Butterworth band-pass filter or high-pass filter. The later was used in this research as a homomorphic filter. This filter accentuates the features and reduces the speckle variations in images.

C. Diffusion Filters

Diffusion filters cancels the noise in images modifying it by solving a partial differential equation. Smoothing depends on the contours present in the image and their directions. Anisotropic diffusion is an efficient nonlinear technique to simultaneously enhance the contrast and reduce the noise level. It smoothens homogeneous regions and keeps contours unchanged without the need of the image power spectrum. Therefore, this filter can be applied on logarithmic compressed images.

1) Anisotropic diffusion filter

Function $d_{i,j,t} = f(|\nabla g|)$ is considered for smoothing the original image while keeping high intensity discontinuities unchanged:

$$\frac{dg_{i,j,t}}{dt} = div\left[d_{i,j,t}\nabla g_{i,j,t}\right] = \\ = \left[\frac{d}{di}d_{i,j,t}\frac{d}{di}g_{i,j,t}\right] + \left[\frac{d}{dj}d_{i,j,t}\frac{d}{dj}g_{i,j,t}\right] \quad (9)$$

where $|\nabla g|$ is the gradient magnitude and $d(|\nabla g|)$ is a contour stopping function which is selected to satisfy the condition $d \to 0$ when $|\nabla g| \to \infty$, such as diffusion is stopped on those contours. The $cd|\nabla g|$ function, called *diffusion coefficient*, is a monotonous decreasing function of the gradient magnitude $|\nabla g|$, leading to intra-region smoothing and keeping inter-region unchanged by preventing diffusion on image contours. An anisotropic partial difference equation is given by (9). Two diffusion coefficients are proposed:

$$cd|\nabla g| = \frac{1}{1+\left(\frac{\nabla g_{i,j}}{K}\right)^2}, \quad (10)$$

$$cd|\nabla g| = \frac{2|\nabla g_{i,j}|}{2+\left(\frac{\nabla g_{i,j}}{K_1}\right)^2}, \quad (11)$$

where K and K_1 are threshold parameters of the positive gradient, known as *diffusion coefficients*. This study considers only the first of the coefficients as it provides better results.

A discrete definition of the anisotropic diffusion given in (9) is as follows:

$$\frac{dg_{i,j}}{dt} = \frac{\lambda}{\eta_s}\left\{d_{i+1,j,t}\left[g_{i+1,j} - g_{i,j}\right] + d_{i-1,j,t}\left[g_{i-1,j} - g_{i,j}\right] + \right. \\ \left. + d_{i,j+1,t}\left[g_{i,j+1} - g_{i,j}\right] + d_{i,j-1,t}\left[g_{i,j-1} - g_{i,j}\right]\right\} \quad (12)$$

where the new gray level intensity of pixel $f_{i,j}$, at position i, j is:

$$f_{i,j} = g_{i,j} + \frac{1}{2}\frac{dg_{i,j}}{dt}, \quad (13)$$

where $d_{i+1,j,t}$, $d_{i-1,j,t}$, $d_{i,j+1,t}$ and $d_{i,j-1,t}$ are the diffusion coefficients for west, east, north and south directions, respectively, in a 4-vecinity surrounding the central pixel i, j where diffusion is computed.

For regions with higher intensity differences between neighbors the diffusion coefficient is also higher, leading to accentuated smoothing, while the opposite is true for regions with lower intensity differences between neighbors.

Constant $\lambda \in R^2$ is a scalar that determine diffusion rate, while η_s is the spatial neighborhood of pixel i, j, and $|\eta_s|$ is the count of neighbor pixels (usually 4 pixels, excepting the image limits). A linear approximation of the directive derivative is considered, such as $\nabla g_{i,j} = g_{i+1,j} - g_{i,j}$ for the eastern direction of central pixel i, j. The anisotropic filter parameters used in this study are: 20 iterations, $\lambda = 0.25$, $\eta_s = 4$ and feature K used for contour stopping function $cd(|\nabla g|)$ is considered as 30.

2) Anisotropic nonlinear coherent diffusion filter

This filter uses a symmetrically positive semi-defined diffusion tensor with parameters defined by (14)

$$\frac{dg_{i,j,t}}{dt} = div\left[D\nabla g\right], \quad (14)$$

where $D \in R^2$ is a positive symmetrically semi-defined diffusion tensor representing the required diffusion in the gradient and contour directions, therefore enhancing both the coherent structures and contours. The definition of D and the derivative of the coherent nonlinear anisotropic diffusion model are defined as follows:

$$D = \begin{pmatrix}\omega_1 & \omega_2\end{pmatrix}\begin{pmatrix}\lambda_1 & 0 \\ 0 & \lambda_1\end{pmatrix}\begin{pmatrix}\omega_1^T \\ \omega_2^T\end{pmatrix}, \quad (15)$$

with

$$\lambda_1 = \begin{cases}\alpha\left(1 - \frac{(\mu_1 - \mu_2)^2}{s^2}\right), & \text{if } (\lambda_1 - \lambda_2)^2 \le s^2 \\ 0, & \text{otherwise}\end{cases}, \quad \lambda_2 = \alpha, \quad (16)$$

where the eigenvectors ω_1, ω_2 and eigenvalues λ_1, λ_2 of η_s correspond to the maximum and minimum difference of direction and resistance to this variation. The flux in each pixel is influenced by local coherence, which is measured using $(\mu_1 - \mu_2)$ in (16). The filter parameters used in this study are: $s^2 = 2$ and $\alpha = 0.9$, diffusion tensor D, and $m = 0.2$ defines the diffusion steps. Local coherence is close to zero in very noisy regions and diffusion gets isotropic $(\mu_1 = \mu_2 = \alpha = 0.9)$, while for lower noise levels the local coherence is $(\mu_1 - \mu_2)^2 > s^2$. The number of iterations considered for each image in this study is 5.

D. Wavelet Filters

The use of spectral filtering for speckle cancelation is based on the use of Daubechie Symlets and fine tuning. Their use was first proposed in [21] and further investigated in [18], [22]. The Symlet family of function, although not perfect, was designed to have the lowest asymmetry and the highest number of zero crossings [21].

III. METHODOLOGY

In this section are presented the database, the ultrasound scanner used for image acquisition, as well as several measures for image quality in order to evaluate the quality difference between original and anti-speckle filtered images.

A. Database and ultrasound image acquisition

In this study 31 ultrasound images were used representing ultrasound carotid bifurcation atherosclerosis. These images are acquired as part of a diagnosis service with the *Vivid i* ultrasound scanner produced by General Electric. The scanner is equipped with high resolution 2.2-5 *MHz*

bandwidth, a 18×24 *mm* acoustic aperture. All images were acquired according those images shown on the scanner display after logarithmic compression. All images are stored on a SSD with a 1024×768 pixels resolution and 256 levels.

B. Image quality measures

The quality of medical images can be objectively defined in terms of performance in relevant clinic tasks, such as lesions detection and classification, anomaly detection, feature estimation, or a combination of them [23]. Most studies have evaluated the equipment performance by testing the diagnose performance of several clinic experts which admit the intra- and inter-observer variability. Although the most important technique of image degradation, several studies have tried to evaluate the actual size of physical degradations [24]. The image quality is of high importance when atherosclerotic carotid is evaluated or segmented [25] or the carotid artery intima-media-complex [26], where the speckle is hiding subtle details in images [8,10] din imagine. A recent study [10] claims that the speckle reduction in images increases the medical expert visual perception when evaluating the carotid artery ultrasound images.

When the speckle is evident in images, various medical expert noise observations constrains different weights of the artifact [23]. Researchers have claimed that both specialists and non-specialists study various critical features in images in order to develop a personal view related to the image quality [10]. Therefore, to evaluate the anti-speckle filtering image quality measures can be used.

Differences between original $g(i,j)$ and anti-speckle filtered images $f(i,j)$ have been evaluated using image quality measures. The following measures with physical meaning can be estimated [9], [10]:

- Mean Square Error (MSE) [10].
- Root Mean Square Error (RMSE), which is the square root of the MSE in a M×N window [10].
- Minkowski metric sum of error (Err3, Err4), which is the dissimilarity measure between original and anti-speckle filtered images [10], [24].
- Geometric Average Error (GAE) [10], [23].
- Signal to Noise Ratio (SNR) [10].
- Peak SNR (PSNR) [10].
- Universal quality index (Q) [27] which models any deformity as a combination of three different values: correlation loss, luminance distortion and contrast distortion.
- Structural Similarity Index (SSIN) between two images [24], as a generalization of Q.

IV. Experimental Results

This chapter presents the results obtained using the ten filters presented in Chapter II on each of the 31 ultrasound images. Nine image quality features have been computed.

A. Results of anti-speckle image filtering

Figures show an ultrasound image of a carotid artery as well as the anti-speckle filtered versions.

Best visual results evaluated by two experts [20] are obtained using the *first order statistics* and *local homogeneous mask* filters, while the *geometric*, *anisotropic diffusion* and *anisotropic nonlinear coherent diffusion* filters show good results but considerably smoothen the image, therefore discarding some subtle details in images. Blurry images are created by the *median*, *Wiener*, *homogeneous neighbor pixel* and *wavelet* filters.

B. Image quality measures

Table II shows the results of image quality measures for the 31 ultrasound images from the database by comparing the original and anti-speckle images. The best results are obtained using the *first order statistics*, a*nisotropic nonlinear coherent diffusion* and *Wiener* filters, with the lowest values for MSE, RMSE, Err3 and Err4 and the highest values for SNR and PSNR. GAE is always zero, as it can be considered that the information remains unchanged from the original in the filtered images. Best values of Q and SSIN are obtained by using the *first order statistics* and *median* filters.

V. Conclusion

The anti-speckle filtering is heavily studied in the latest years. The present research presents the main principles, the theoretical background and the algorithms as a representative group of anti-speckle filters. Moreover, some specific anti-speckle filtering applications have been shown, with a great variety of ultrasound image processing.

The *Wiener* filter can be used to increase the optical perception in ultrasound images but, comparing with the *first order statistics* filter, it does not retain the contours. Moreover, it is not appropriate to be used as a statistical analysis and for increasing the classification accuracy. The *local homogeneous mask* filter is suitable for increasing the statistical analysis and classification precision, but it does not conserve contours and global quality in images. The *median* filter is more suitable for increasing the optical perception, but repetitive filtering contours in images. The *homogeneous neighbor pixel* filter is used to enhance the classification of organs and tissues and also to enhance contours, therefore increasing the optical perception. The *geometric* filter has very good results for noise speckle reduction in images.

The *homomorphic* filters enhance features and reduce speckle variations in images. The *anisotropic diffusion* usually consistently smoothens contours in images but it can also be used to increase video coding quality and reduces the bandwidth required for image transmission in wireless networks [29]. The *anisotropic nonlinear coherent diffusion* filter can be used to increase the visual appearance of clinic structures and to enhance the atherosclerotic carotid plaque contours in ultrasound images [25].

The anti-speckle filtering is an important step for enhancing ultrasound images of carotid arteries. This paper shows the simple filters based on local statistics (*first order statistics* and *local homogeneous mask*) and *geometric* filters could be successfully used to process ultrasound images. Therefore, anti-speckle filtering can be used as a pre-processing for automatic segmentation of the Intimal-Medial Thickness [28] and the carotid plaque, followed by texture analysis and classification of carotid plaque. Despite, further research is required in order to evaluate at a larger scale the

anti-speckle filters presented, as well as their impact in clinical practice. Moreover, the utility of the proposed anti-speckle filters in portable ultrasound systems and wireless telemedicine must still be investigated.

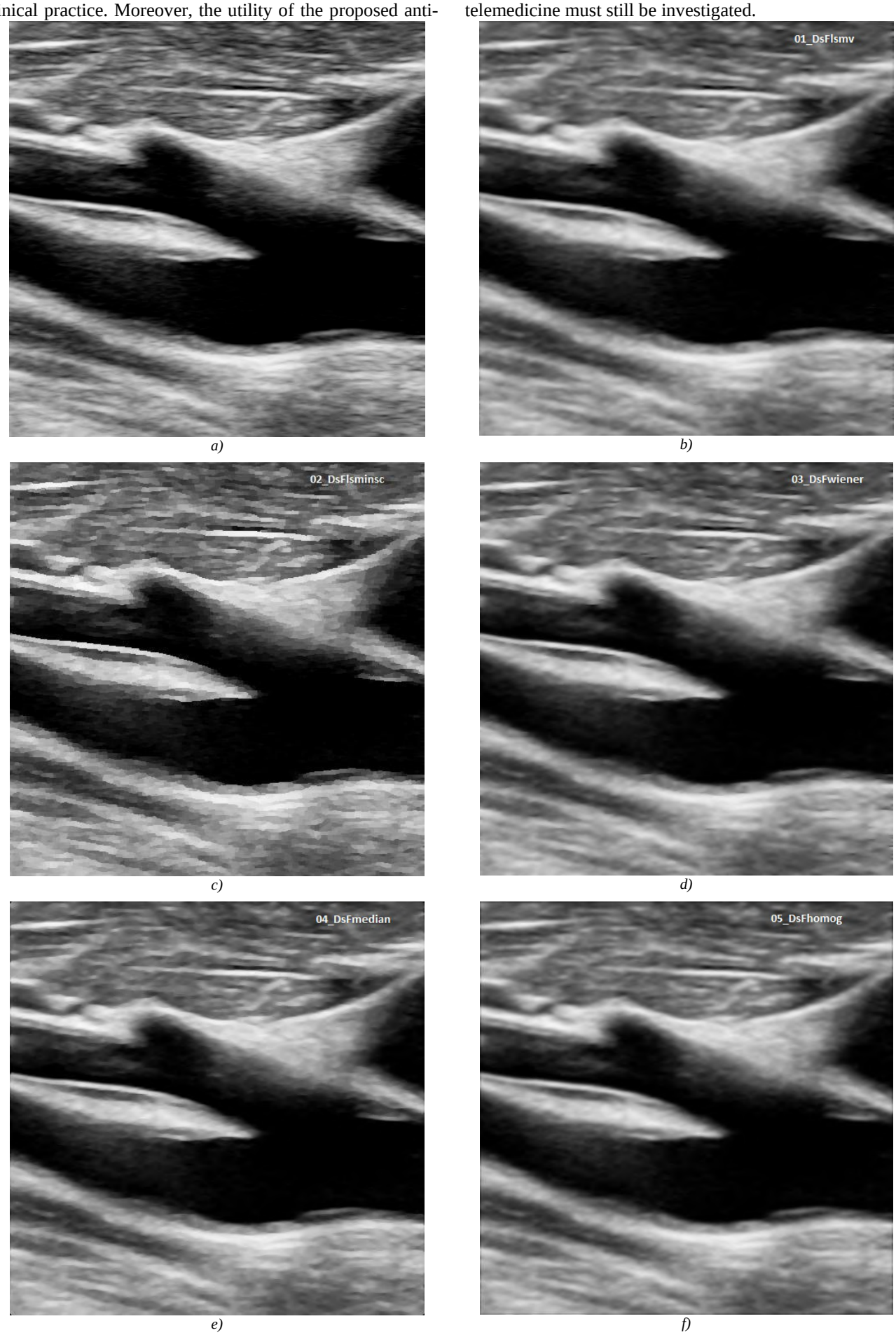

a) *b)* *c)* *d)* *e)* *f)*

Figure 3. Filters applied on: *a*) original image, *b*) linear filter, *c*) homogeneous mask filter, *d*) Wiener filter, *e*) median filter, *f*) homogeneous filter

g)

h)

i)

j)

k)

l)

Figure 3 (*cont.*). *g*) original, *h*) geometric filter, *i*) homomorphic filter, *j*) anisotropic diffusion filter, *k*) coherent nonlinear diffusion filter, *l*) wavelet filter

TABLE II. QUALITY MEASURES OF ANTI-SPECKLE FILTERING OF ULTRASOUND CAROTID ARTERY IMAGES

Feature	Linear filters			Non-linear filters				Diffusion filters		Wavelet
	First order statistics	Local homogeneous mask	Wiener	Median	Homogeneous neighbor pixel	Geometric	Homomorphic	Anisotropic diffusion	Anisotropic nonlinear coherent diffusion	Wavelet
MSE	41	113	41	41	56	479	50	381	37	126
RMSE	6	11	6	6	7	22	7	19	6	11
Err3	8	15	7	8	9	31	9	25	7	12
Err4	9	19	8	12	11	40	14	32	8	13
GAE	0	0	0	0	0	0	0	0	0	0
SNR	27	22	27	27	26	16	26	18	28	22
PSNR	35	30	36	35	34	24	34	25	36	30
Q	0.88	0.84	0.84	0.88	0.83	0.62	0.83	0.56	0.78	0.73
SSIN	0.92	0.88	0.91	0.93	0.90	0.73	0.91	0.73	0.91	0.77

REFERENCES

[1] S. H. Contreras Ortiz, Tsuicheng Chiu, M. D. Fox, "Ultrasound image enhancement: A review", *Biomedical Signal Processing and Control*, vol. 7, no. 5, pp. 419-428, Sep., 2012. doi: 10.1016/j.bspc.2012.02.002

[2] J. W. Goodman, *Speckle Phenomena in Optics: Theory and Applications*, Roberts & Co, 2007.

[3] R. F. Wagner, S. W. Smith, J. M. Sandrik, H. Lopez, "Statistics of Speckle in Ultrasound B-Scans," *IEEE Transactions on Sonics and Ultrasonics*, vol. 30, no. 3, pp.156-163, May, 1983. doi: 10.1109/T-SU.1983.31404

[4] K. Z. Abd-Elmoniem, A.-B. Youssef, Y. M. Kadah, "Real-time speckle reduction and coherence enhancement in ultrasound imaging via nonlinear anisotropic diffusion," *IEEE Transactions in Biomedical Engi*neering, vol. 49, no. 9, 2002, pp. 997-1014. doi: 10.1109/TBME.2002.1028423

[5] V. Dutt, "Statistical analysis of ultrasound echo envelope," Ph.D. dissertation, Mayo Graduate School, Rochester, MN, 1995.

[6] C. P. Loizou, C. S. Pattichis, "Despeckle filtering algorithms and software for ultrasound imaging," Morgan & Claypool, 2008. doi: 10.2200/S00116ED1V01Y200805ASE001

[7] Y. Yongjian, S. T. Acton, "Speckle reducing anisotropic diffusion," *IEEE Trans. Image Process.*, vol. 11, no. 11, pp. 1260-1270, Nov., 2002. doi: 10.1109/TIP.2002.804276

[8] C. P. Loizou et al., "Despeckle filtering in ultrasound imaging of the carotid artery," in *Advances in Diagnostic and Therapeutic Ultrasound Imaging*, J. S. Suri, C. Kathuria, R.-F. Chang, F. Molinari, A. Fenster, Editors, Artech House, 2005, pp. 37-63.

[9] C. P. Loizou, C. S. Pattichis, M. Pantziaris, T. Tyllis, and A. Nicolaides, "Quality evaluation of ultrasound imaging in the carotid artery based on normalization and speckle reduction filtering," *Medical and Biological Engineering and Computing*, 44:414, 2006. doi: 10.1007/s11517-006-0045-1

[10] C. P. Loizou, C. S. Pattichis, "Despeckle filtering Algorithms and Software for Ultrasound Imaging," *San Rafael: Morgan & Claypool*, 2008. doi: 10.2200/S00116ED1V01Y200805ASE001

[11] L. J. Busse, T. R. Crimmins, J. R. Fienup, "A model based approach to improve the performance of the geometric filtering speckle reduction algorithm," in Proc. IEEE Ultrasonics Symposium, pp. 1353-1356, Seattle, USA, Nov. 7-10, 1995. doi: 10.1109/ULTSYM.1995.495807

[12] M. F. Insana, T. J. Hall, G. G. Cox, S. J. Rosenthal, "Progress in Quantitative Ultrasonic Imaging," in Proc. SPIE 1090 on Medical Imaging III: Image Formation, pp. 1092-1099, May, 1989. doi: 10.1117/12.953184

[13] V. S. Frost, J. A. Stiles, K. S. Shanmugan, J. C. Holtzman, "A Model for Radar Images and Its Application to Adaptive Digital Filtering of Multiplicative Noise," *IEEE Transactions on Pattern Analysis and Machine Intelligence*, vol. PAMI-4, no. 2, pp. 157-166, Mar., 1982. doi: 10.1109/TPAMI.1982.4767223

[14] J.-S. Lee, "Refined filtering of image noise using local statistics," Computer Graphics and Image Processing, vol. 15, no. 4, pp. 380-389, Apr., 1981. doi: 10.1016/S0146-664X(81)80018-4

[15] S. Solbo, T. Eltoft, "Homomorphic wavelet-based statistical despeckling of SAR images," *IEEE Transactions on Geoscience and Remote Sensing*, vol. 42, no. 4, pp. 711-721, Apr., 2004. doi: 10.1109/TGRS.2003.821885

[16] J. Saniie, T. Wang, N. Bilgutay, "Analysis of homomorphic processing for ultrasonic grain signal characterization," *IEEE Transactions on Ultrasonics, Ferroelectrics, and Frequency Control*, vol. 36, no. 3, May, 1989. doi: 10.1109/58.19177

[17] K. Z. Abd-Elmoniem, A. B. M. Youssef, Y. M. Kadah, "Real-time speckle reduction and coherence enhancement in ultrasound imaging via nonlinear anisotropic diffusion," *IEEE Transactions on Biomedical Engineering*, 2002. doi: 10.1109/TBME.2002.1028423

[18] S. Zhong, V. Cherkassky, "Image denoising using wavelet thresholding and model selection," in Proc. *IEEE International Conference on Image Processing*, Sep. 10-13, 2000. doi: 10.1109/ICIP.2000.899345

[19] M. Nagao, T. Matsuyama. "Edge preserving smoothing," *Computer Graphics and Image Processing*, vol. 9, no. 4, pp. 394-407, Apr., 1979. doi: 10.1016/0146-664X(79)90102-3

[20] A. Nicolaides, K. W. Beach, E. Kyriacou, C. S. Pattichis Editors, *Ultrasound and Carotid Bifurcation Atherosclerosis*, Springer-Verlag London, 2012. doi: 10.1007/978-1-84882-688-5

[21] D. L. Donoho, "Denoising by soft thresholding," *IEEE Transactions on Information Theory*, vol. 41, no. 3, pp. 613-627, May, 1995. doi: 10.1109/18.382009

[22] S. Gupta, R. C. Chauhan, S. C. Sexana, "Wavelet-based statistical approach for speckle reduction in medical ultrasound images," *S.C. Med. Biol. Eng. Comput.*, vol. 42, no. 2, pp. 189-192, Mar., 2004. doi.org/10.1007/BF02344630

[23] S. Winkler, "Vision models and quality metrics for image processing applications," Ph.D. dissertation, EPFL, Lausanne, Switzerland, 2000.

[24] Z. Wang, A. C. Bovik, H. R. Sheikh, E. P. Simoncelli, "Image Quality Assessment: From Error Measurement to Structural Similarity," *IEEE Transactions on Image Processing*, vol. 13, no. 4, pp. 600-612, 2004. doi: 10.1109/TIP.2003.819861

[25] C. P. Loizou, C. S. Pattichis, M. Pantziaris, A. N. Nicolaides, "An Integrated System for the Segmentation of Atherosclerotic Carotid Plaque," *IEEE Trans. Inf. Technol. Biomed.*, vol. 11, no. 6, pp. 661-667, 2007. doi: 10.1109/TITB.2006.890019

[26] C. P. Loizou, C. S. Pattichis, A. N. Nicolaides, M. Pantziaris, "Manual and automated media and intima thickness measurements of the common carotid artery," *IEEE Transactions on Ultrasonics, Ferroelectrics, and Frequency Control*, vol. 56, no. 5, 2009. doi: 10.1109/TUFFC.2009.1130

[27] Z. Wang, A. C. Bovik, "A universal image quality index," *IEEE Signal Processing Letters*, vol. 9, no. 3, Mar. 2002. doi: 10.1109/97.995823

[28] C. P. Loizou, C. S. Pattichis, M. Pantziaris, A. N. Nicolaides, T. Tyllis, "Snakes based segmentation of the common carotid artery intima media." *Med.&Biol. Eng. Comput.*, vol. 45, no. 1, pp. 35-49, 2007. doi: 10.1007/s11517-006-0140-3

[29] A. Panayides, M. S. Pattichis, C. S. Pattichis, C. P. Loizou, M. Pantziaris, A. Pitsillides, "Atherosclerotic plaque ultrasound video encoding, wireless transmission, and quality assessment using H.264," *IEEE Trans. Inform. Technol. Biomed.*, vol. 15, no. 3, pp. 387-397, 2001. doi: 10.1109/TITB.2011.2105882